Monthly Notices of the ROYAL ASTRONOMICAL SOCIETY

MNRAS **437,** 3124–3132 (2014) doi:10.1093/mnras/stt2052
Advance Access publication 2013 December 5

The effect of toroidal magnetic field on the thickness of a viscous–resistive hot accreting flow

M. Samadi,[1]★ S. Abbassi[1,2]★ and M. Khajavi[1]

[1]*Department of Physics, School of Sciences, Ferdowsi University of Mashhad, Mashhad 91775-1436, Iran*
[2]*School of Astronomy, Institute for Studies in Theoretical Physics and Mathematics, PO Box 19395-5531, Tehran, Iran*

Accepted 2013 October 21. Received 2013 October 21; in original form 2013 August 12

ABSTRACT

By taking into account the effect of a toroidal magnetic field and its corresponding heating, we determine the thickness of advection-dominated accretion flows. We consider an axisymmetric, rotating, steady viscous–resistive, magnetized accretion flow under an advection-dominated stage. The dominant mechanisms of energy dissipation are assumed to be turbulence viscosity and magnetic diffusivity. We adopt a self-similar assumption in the radial direction to obtain the dynamical quantities, i.e. radial, azimuthal, sound and Alfvén velocities. Our results show that the vertical component of magnetic force acts in the opposite direction to gravity and compresses the disc; thus, compared with the non-magnetic case, in general the disc half-thickness, $\Delta\theta$, is significantly reduced. On the other hand, two parameters that appear due to the action of the magnetic field and reaction of the flow affect the disc thickness. The first one, β_0, which shows the magnetic field strength at the equatorial plane, decreases $\Delta\theta$. The other one, η_0, is the magnetic resistivity parameter and when it increases $\Delta\theta$ also increases.

Key words: accretion, accretion discs – black hole physics – magnetic fields – MHD.

1 INTRODUCTION

Accretion on to black holes is known as a powerful source of energy in the Universe. Accreting gas with sufficiently high angular momentum tends to form a disclike structure around the central object. In accreting processes, viscosity causes angular momentum transport outward and it also releases gravitational energy. According to the standard accretion disc model, the released energy is converted into radiation and escapes from the disc in the same place as its generation. The modern standard theory was formulated in Shakura (1972), Novikov & Thorne (1973) and Shakura & Sunyaev (1973). It provided remarkably successful contributions to understanding quasars, X-ray binaries and active galactic nuclei. One of the basic assumptions of this model is that the vertical thickness of the disc H is much smaller than the corresponding radius r in cylindrical coordinates ($H \ll r$). Although the disc is geometrically thin, it is optically thick due to absorption and radiation in its entirety moves outward in the vertical direction.

On the other hand, the energy released through viscosity may be trapped within accreting gas and then transported (advected) in the radial direction towards the central object or stored in the flow as entropy (Narayan & Yi 1995b). In this case, the gas tends to have higher temperature, which leads to a vertical thickening of the disc ($H \sim R$). In this situation, therefore, the accretion flow is called a radiatively inefficient accretion flow (RIAF) and depending on the mass accretion rate and optical depth of flow is divided into two types, namely the slim disc and the advection-dominated accretion flow (ADAF). The slim accretion disc model, where flow is optically thick because of having a large mass accretion rate, is introduced by Abramowicz et al. (1988). In the other type, ADAF, the accreting flow becomes optically thin in the limit of low mass accretion rate.

For both branches of hot accretion flows, the solution proposed by Narayan & Yi (1994) is applicable. Using a self-similar technique, they assumed all variables to have power-law dependence on r and then started to integrate the flow equations in the vertical direction. However, vertical integration is valid for the thin disc approximation only. Thus Narayan & Yi (1995a) tried to obtain a new solution in spherical coordinates to approach a more exact model. At that time, the flow was considered completely thick and occupied the whole region between the two poles. In both solutions the thickness value of the flow is not entirely clear.

It is generally believed that magnetic fields have a fundamentally important role in the physics of accretion discs. For example, magnetorotational instability (MRI) is known as a sure generator of turbulence in a Keplerian disc, where angular momentum decreases outwards (Balbus & Howly 1991). Indeed, the crucial role of the magnetic field in a hot flow is expected because of the high temperature of accreting gas in ADAFs (10^9–10^{12} K). In this case, the flow is ionized and may be influenced strongly in the presence of a magnetic field. For the first time, Lynden-Bell (1969) considered the role of the magnetic field in the context of active galactic nuclei

★E-mail: m_samadi_m@yahoo.com (MS); abbassi@ipm.ir (SA)

and found how it might be responsible for angular momentum transport and the origin of anomalous disc viscosity. Bisnovatyi-Kogan & Blinnikov (1976) demonstrated that an explanation for the hard X-ray and gamma radiation from Cyg X-1 would require the presence of a magnetic field in the accretion disc. Some effort has been made to solve the magnetohydrodynamics (MHD) equations of magnetized ADAFs analytically. Kaburaki (2000) has presented a set of analytical solutions for a fully advective accretion flow in a global magnetic field. Shadmehri (2004) has extended this analysis for a non-constant resistivity. Abbassi, Ghanbari & Ghasemnezhad (2010) and Ghanbari, Salehi & Abbassi (2007) have presented a set of self-similar solutions for two-dimensional (2D) viscous–resistive ADAFs in the presence of a dipolar magnetic field of the central object. They have shown that the presence of a magnetic field and its associated resistivity can change the picture considerably with regard to accretion flows.

The effects of ordered magnetic fields in accretion disc theories are often studied in two classes. In one class, the magnetic field is global and both poloidal and toroidal components of the ordered field are considered. In the other class, only a toroidal field is present in the disc. The latter case is acceptable, since the dominant motion in an accretion disc has differential rotation, so it causes the toroidal component of magnetic field to become the most important one. Toroidal field is created by the action of differential rotation on initially poloidal field lines connecting layers rotating at different rates (Papaloizou & Terquem 1997). In this class, the magnetic field is often assumed to have even polarity, which means being the same on both sides of the equatorial plane, and its effect is usually seen in the total pressure (i.e. gas plus magnetic). In this view, therefore, the behaviour of magnetic and gas pressure are assumed to be the same and both support the disc against the vertical component of gravity. Therefore, if the total pressure is substituted in the α-prescription of viscosity, an additional viscous extraction of angular momentum passing through the disc plane becomes possible (Kato, Fukue & Mineshige 2008). The effect of toroidal magnetic field on the disc was studied by Fukue (1990), Akizuki & Fukue (2006), Abbassi, Ghanbari & Najjar (2008), Abbassi et al. (2010) and Khesali & Faghei (2009).

The global magnetic field could have odd or even symmetry about the equatorial plane. Lovelace et al. (1986) and Lovelace, Wang & Sulkanen (1987) proposed a general theory for axisymmetric flows around a black hole in a cylindrical (r, ϕ, z) coordinate system and showed that, in the presence of a magnetic field, the magnetic force can affect the thickness of the accretion disc. Wang, Sulkanen & Lovelace (1990) considered a viscous–resistive accretion disc in the presence of a global magnetic field. By using the thin disc approximation, they have concluded that, in odd symmetry about the equatorial plane, $z = 0$ ($B_z(r, z) = -B_z(r, -z), B_r(r, z) = B_r(r, -z), B_\phi(r, z) = B_\phi(r, -z)$; note that here B_ϕ is even symmetry), the vertical component of magnetic force is opposed by gravity but in the case with even symmetry the magnetic force is a compressive force like gravity. Nevertheless, if the magnetic field is purely toroidal with an odd configuration, the magnetic force will compress the disc (see Campbell & Heptinstall 1998; Liffman & Bardou 1999, for details).

The thickness of an advection-dominated disc is not well defined. There is just a rough approximation used in the α-prescription (i.e. $H/r = c_s/v_K$, where c_s is the sound velocity at the disc equator and v_K is the Keplerian velocity), in height-integrated cylindrical coordinate solutions or even in the spherical solutions presented by Narayan & Yi (1995a , hereafter NY95). Overcoming this problem, Gu et al. (2009, hereafter GXLL09) introduced a somewhat different way to estimate the flow thickness. They did not give the value of $f = Q_{adv}/Q_{vis}$ (here, Q_{adv} is the advective cooling rate per unit area and Q_{vis} the viscous heating rate per unit area) in advance, but instead considered accretion flows with free surfaces. The boundary condition is set to $p = 0$, which is usually adopted in the literature (e.g. Kato et al. 2008). Thus the thickness of the disc $\Delta\theta$ makes sense and they calculated f to see how it relates to $\Delta\theta$.

In this article we aim to estimate the thickness of an advection-dominated disc in the presence of a purely toroidal magnetic field using the GXLL09 method.

The outline of this article is as follows. In Section 2 we present the basic magnetohydrodynamics equations, which include the induction equation with non-constant magnetic resistivity. Self-similar equations are investigated in Section 3. In Section 4, we explain a new view of the advection parameter. The results of the numerical solution and a derivation of the disc thickness are presented in Section 5 and, finally, discussions and conclusions are given in Section 6.

2 BASIC EQUATIONS

In this article, we consider a steady-state ($\partial/\partial t = 0$) axisymmetric ($\partial/\partial\phi = 0$) hot accretion flow. Spherical coordinates are used (r, θ, ϕ). The gravitational field emanates only from a central point mass and we neglect self-gravity of the accreting flow. We also neglect relativistic effects. The basic equations of the system are composed of the continuity, momentum and induction equations. The equation of continuity is

$$\frac{\partial \rho}{\partial t} + \nabla \cdot (\rho \boldsymbol{V}) = 0, \tag{1}$$

the equation of momentum conservation is

$$\rho \frac{\mathrm{D}\boldsymbol{V}}{\mathrm{D}t} = -\nabla p - \rho \nabla \Phi + \boldsymbol{F}^{\nu} + \frac{1}{c}(\boldsymbol{J} \times \boldsymbol{B}), \tag{2}$$

where $\mathrm{D}/\mathrm{D}t = \partial/\partial t + \boldsymbol{V} \cdot \nabla$, and, finally, Faraday's law of induction becomes

$$\frac{\partial \boldsymbol{B}}{\partial t} = \nabla \times (\boldsymbol{V} \times \boldsymbol{B}) - \nabla \times (\eta \nabla \times \boldsymbol{B}), \tag{3}$$

where ρ, p, $\boldsymbol{V}$ and $\boldsymbol{B}$ are the density of the gas, the pressure, the time-averaged flow velocity and the time-averaged magnetic field, respectively. These equations are supplemented by the Maxwell equations, $\nabla \times \boldsymbol{B} = 4\pi \boldsymbol{J}/c$, and by $\nabla \cdot \boldsymbol{B} = 0$. Here, η is the magnetic diffusivity, $\boldsymbol{F}^{\nu} = -\nabla \cdot \boldsymbol{T}^{\nu}$ is the viscous force, with $T^{\nu}_{jk} = -\rho\nu(\partial v_j/\partial x_k + \partial v_K/\partial x_j - (2/3)\delta_{jk}\nabla \cdot \boldsymbol{V})$ (in Cartesian coordinates), and ν is the kinematic viscosity. We assume that only the $r\phi$-component of the viscous stress tensor, $T_{r\phi}$, is important. In spherical coordinates, continuity and the three components of the momentum equation can be written respectively as

$$\frac{1}{r^2}\frac{\partial}{\partial r}(r^2 \rho v_r) + \frac{1}{r \sin\theta}\frac{\partial}{\partial \theta}(\sin\theta \rho v_\theta) = 0, \tag{4}$$

$$v_r \frac{\partial v_r}{\partial r} + \frac{v_\theta}{r}\frac{\partial v_r}{\partial \theta} - \frac{1}{r}(v_\theta^2 + v_\phi^2) = -\frac{GM}{r^2} - \frac{1}{\rho}\frac{\partial p}{\partial r} + \frac{1}{c\rho}(J_\theta B_\phi - J_\phi B_\theta), \tag{5}$$

$$\frac{v_r}{r}\frac{\partial (r v_\theta)}{\partial r} + \frac{v_\theta}{r}\frac{\partial v_\theta}{\partial \theta} - \frac{v_\phi^2}{r}\cot\theta = -\frac{1}{r\rho}\frac{\partial p}{\partial \theta} + \frac{1}{rc\rho}(J_\phi B_r - J_r B_\phi), \tag{6}$$

$$\frac{v_r}{r}\frac{\partial(rv_\phi)}{\partial r}+\frac{v_\theta}{r\sin\theta}\frac{\partial}{\partial\theta}(\sin\theta v_\phi) = \frac{1}{\rho r^3}\frac{\partial}{\partial r}(r^3T_{r\phi})+\frac{1}{c\rho}(J_rB_\theta-J_\theta B_r), \quad (7)$$

where v_r, v_θ and v_ϕ are the three velocity components. Here the induction equation is considered.

We suppose a toroidal magnetic field $\boldsymbol{B}=B_\phi\hat{\phi}$ (which satisfies $\nabla\cdot\boldsymbol{B}=0$ with the axisymmetric assumption); therefore, the components of current density, $\boldsymbol{J}$, become

$$J_r=\frac{c}{4\pi r}\frac{1}{\sin\theta}\frac{\partial}{\partial\theta}(\sin\theta B_\phi),\quad J_\theta=-\frac{c}{4\pi r}\frac{\partial}{\partial r}(rB_\phi),\quad J_\phi=0.$$

NY95 assumed $v_\theta=0$, which implies that no accretion material can evaporate as outflow from the discs. Here, following NY95 for simplicity, we adopt $v_\theta=0$ because at this stage we are interested in studying possible effects of the B field on the vertical structure of the discs although, in a more realistic picture, $v_\theta\neq0$ should be taken into account (Xue & Wang 2005). By substituting the current density relation, J, the magnetic field $\boldsymbol{B}=B_\phi\hat{\phi}$ and also $v_\theta=0$, the continuity and momentum equations (4)–(7) reduce to

$$\frac{1}{r^2}\frac{\partial}{\partial r}(r^2\rho v_r)=0, \quad (8)$$

$$v_r\frac{\partial v_r}{\partial r}-\frac{v_\phi^2}{r}=-\frac{GM}{r^2}-\frac{1}{\rho}\frac{\partial p}{\partial r}-\frac{1}{4\pi\rho}\frac{B_\phi}{r}\frac{\partial}{\partial r}(rB_\phi), \quad (9)$$

$$v_\phi^2\cot\theta=\frac{1}{\rho}\frac{\partial p}{\partial\theta}+\frac{1}{4\pi\rho}\left[\frac{B_\phi}{\sin\theta}\frac{\partial}{\partial\theta}(\sin\theta B_\phi)\right], \quad (10)$$

$$v_r\frac{\partial(rv_\phi)}{\partial r}=\frac{1}{\rho r^2}\frac{\partial}{\partial r}(r^3T_{r\phi}). \quad (11)$$

The $r\phi$ component of the viscous stress tensor is defined by $T_{r\phi}=\rho\nu r\partial(v_\phi/r)/\partial r$. For the viscosity, ν, we will use the α-prescription so $\nu=\alpha c_s^2 r/v_K$, where α is the constant viscosity parameter, c_s is the sound speed defined as $c_s^2=p/\rho$, and $v_K^2=GM/r$ is the Keplerian velocity.

The induction equation has three components; only its azimuthal component remains, since a toroidal magnetic field configuration is assumed. Since we assume steady flows, then $\partial B_\phi/\partial t=0$, so we have

$$\frac{1}{r}\frac{\partial}{\partial r}\left[\eta\frac{\partial(rB_\phi)}{\partial r}-rv_rB_\phi\right]+\frac{1}{r^2}\frac{\partial}{\partial\theta}\left[\frac{\eta}{\sin\theta}\frac{\partial}{\partial\theta}(\sin\theta B_\phi)\right]=0. \quad (12)$$

It is clear that the above equations are nonlinear and we are not able to solve them analytically. Therefore, it is useful to have a simple means to investigate the properties of solutions.

Self-similar methods have been very useful in astrophysics and are widely adopted in the astrophysical literature, since the similarity assumption reduces the complexity of the partial differential equations. This technique was applied by Narayan & Yi (1994) in order to solve the system of height-averaged equations of a hot accreting flow. They then investigated numerically the range of validity of their self-similar solutions. Their results show that over a range of intermediate radii the numerical solution is close to the self-similar form, e.g. in a typical case this range is $10r_{in}<r<10^{-2}r_{out}$, where r_{in} is the inner edge and r_{out} is the outer edge of the disc.

We will present self-similar solutions of these equations in the next section.

3 SELF-SIMILAR SOLUTIONS

The main equations are a set of coupled differential equations and thus they require a numerical solution. However, there is a powerful technique to give an approximate solution. This powerful technique is the self-similar method, a dimensional analysis and scaling law, which is a common tool in astrophysical fluid mechanics. Similar to NY95, we assume self-similarity in the radial direction so all types of velocities are proportional to $r^{-1/2}$ and for density $\rho\propto r^{-3/2}$ and therefore the gas and magnetic pressure must be $(p, B_\phi^2)\propto r^{-5/2}$. If we adopt the above self-similar scaling, in fact, the radial dependences of all physical quantities are cancelled out and a set of equations remains in which all quantities just are a function of θ. If we put these self-similar relations in the continuity equation, no new result is achieved, but the other equations become

$$v_\phi^2=v_K^2-\frac{1}{2}v_r^2-\frac{5}{2}c_s^2-\frac{1}{4}c_A^2, \quad (13)$$

$$v_\phi^2\cot\theta=\frac{1}{\rho}\frac{\partial\left(\rho c_s^2\right)}{\partial\theta}+c_A^2\cot\theta+\frac{1}{2\rho}\frac{\partial\left(\rho c_A^2\right)}{\partial\theta}, \quad (14)$$

$$v_r=-\frac{3}{2}\frac{\alpha c_s^2}{v_K}. \quad (15)$$

In the above three equations, the gas pressure was replaced by $4\pi\rho c_s^2$ and the square Alfvén velocity, c_A^2, was used instead of $B_\phi^2/4\pi\rho$. Now, in order for terms including B_ϕ^2 and $B_\phi dB_\phi(=dB_\phi^2/2)$ in equation (12) to appear, we first multiply by B_ϕ and then use self-similar relations, yielding

$$\frac{3}{4}\left(\frac{1}{4}\eta+rv_r\right)c_A^2+\frac{\partial\eta}{\partial\theta}\left(v_\phi^2\cot\theta-\frac{1}{\rho}\frac{\partial\left(\rho c_s^2\right)}{\partial\theta}\right)+\eta\left[\frac{\partial v_\phi^2}{\partial\theta}\cot\theta-\frac{v_\phi^2}{\sin^2\theta}-\frac{\partial}{\partial\theta}\left(\frac{1}{\rho}\frac{\partial\left(\rho c_s^2\right)}{\partial\theta}\right)\right]-\frac{\eta}{2}\left(v_\phi^2\cot\theta-\frac{1}{\rho}\frac{\partial\left(\rho c_s^2\right)}{\partial\theta}\right)\left(\frac{1}{c_A^2}\frac{\partial c_A^2}{\partial\theta}-\frac{1}{\rho}\frac{\partial\rho}{\partial\theta}\right)=0. \quad (16)$$

There are six unknown quantities: $\rho, v_r, v_\phi, c_s^2, c_A^2$ and η in four equations (13)–(16), so we need two extra equations. One of them is a relation between pressure and density and the other is a relation for the resistivity. We assume a polytropic relation, $p=k\rho^\gamma$, in the vertical direction (or equvalently meridional direction), where γ is the ratio of specific heats. This is often adopted in vertically integrated models of geometrically slim discs (e.g. Kato et al. 2008). We admit that the polytropic assumption is a simple way to close the system and enable us to calculate the dynamical quantities. We can therefore obtain

$$\frac{1}{\rho}\frac{\partial\rho}{\partial\theta}=\frac{1}{(\gamma-1)c_s^2}\frac{\partial c_s^2}{\partial\theta}. \quad (17)$$

As mentioned above, in order to complete the problem we need to adopt a physical assumption for the magnetic diffusivity. We assume that the magnetic diffusivity is due to turbulence in the accretion flow and it is reasonable to express this parameter in analogy to the α-prescription of Shakura & Sunyaev (1973) for the turbulent viscosity, as follows (Bisnovatyi-Kogan & Ruzmaikin 1976):

$$\eta=\eta_0 r\frac{c_s^2}{v_K}. \quad (18)$$

Now the system is completed and can be solved numerically with proper boundary conditions. We assume that the structure of the disc is symmetric about the equatorial plane, and thus we have

$$\text{at } \theta=\frac{\pi}{2}:\qquad \frac{\partial c_s^2}{\partial\theta}=0,\quad \frac{\partial c_A^2}{\partial\theta}=0.$$

We set $\rho(\theta = \pi/2) = 1$ in order to obtain a unique solution by imposing a characteristic scale density at $\theta = \pi/2$. We need to adopt proper values for c_s^2 and c_A^2 in the equatorial plane. We expect that the disc temperature is maximum in the equator of the disc and therefore $c_s^2(\theta = \pi/2) = c_{s0}^2$ must be maximum there; it will decrease towards the disc surface. By integrating $\partial c_s^2/\partial\theta$ with respect to θ, c_s^2 will decrease to reach zero at angle θ_s for a given c_{s0}^2. We have different θ_s for different c_{s0}^2. Thus, as we expect hotter discs, bigger values of c_{s0}^2 are thick vertically. We need to fix c_A^2 at our inner boundary, $\theta = \pi/2$. Now we may use the familiar relation between gas pressure and magnetic pressure, i.e.

$$\beta = 2\frac{p_m}{p_g} = 2\frac{B_\phi^2/8\pi}{p} = \frac{c_A^2}{c_s^2}. \tag{19}$$

We must emphasize that in this study β is a function of θ, since c_A^2 and c_s^2 are a function of θ, while usually β is assumed constant with respect to θ (Akizuki & Fukue 2006; Abbassi et al. 2008). In the Appendix, we show that B_ϕ^2 is minimum at $\theta = \pi/2$. Since c_s^2, B_ϕ^2 and automatically c_A^2 have opposite behaviour to θ, c_A^2 increases from the equator towards the surface. Using the definition of β, we are able to choose reasonable boundary conditions for c_A^2 and c_s^2. If we consider equation (13) in $\theta = \pi/2$ using the definition of β, (19) and equation (15), we have

$$v_{\phi 0}^2 = v_K^2 - \frac{9\alpha^2}{8v_K^2}c_{s0}^4 - \left(\frac{5}{2} + \frac{\beta_0}{4}\right)c_{s0}^2, \tag{20}$$

where $\beta_0 = \beta(\theta = \pi/2)$ and zero index in the other quantities implies their value in the equatorial plane. It can be deduced that the admissible maximum value of $v_{\phi 0}^2$ is v_K^2. On the other hand, because $v_{\phi 0}^2$ must be positive, the right-hand side of equation (20) must also be positive. Hence we can determine an acceptable interval value of c_{s0}^2 for given β_0, e.g. $0 < c_{s0}^2 < 0.38v_K^2$ for the case $\alpha = 0.1$, $\beta_0 = 0.3$, therefore $c_{A0}^2 = 0.3c_{s0}^2$ is determined; however, as we see, the initial values of both velocities are still arbitrary with just an upper limitation. Now, with the proper boundary conditions, we are able to solve the main equations to deduce the vertical behaviour of the velocities and we can then determine how the magnetic field affects the disc thickness.

4 ADVECTION PARAMETER

In the previous section, without applying an energy equation, we determined velocities and pressures. In order to complete the equation it needs to have an energy equation. In this section we will focus on the energy transport equation. In principle, the general energy equation should be solved and then the advection parameter is obtained as a variable, as done by Manmoto, Mineshige & Kusunose (1997) for ADAFs and by Abramowicz et al. (1988) and Watarai et al. (2000) for slim discs. Following Narayan & Yi (1994), we adopt an advection form for the energy equation ($Q_{adv} = Q_+ - Q_- = fQ_+$), where Q_+, Q_- and Q_{adv} are the heating rate per unit area, the cooling rate per unit area and the advecting cooling rate per unit area, respectively. Here we introduce the advecting heating rate per unit volume as

$$q_{adv} = \rho T\frac{Ds}{Dt} = \rho\frac{De}{Dt} - \frac{p}{\rho}\frac{D\rho}{Dt}. \tag{21}$$

Because we adopt steady-state, axisymmetric flows with $v_\theta = 0$, we have $D/Dt = \boldsymbol{V}\cdot\nabla = v_r\partial/\partial r$. Thus, q_{adv} becomes

$$q_{adv} = \frac{\rho v_r}{\gamma - 1}\frac{\partial c_s^2}{\partial r} - c_s^2 v_r\frac{\partial\rho}{\partial r}. \tag{22}$$

On the other hand, we know $q_{adv} = q_+ - q_-$, where $q_+ = q_{vis} + q_B$ is the dissipation rate per unit value. $q_{vis} = \eta r^2(d\Omega/dr)^2$ and $q_B = J^2/\sigma$ are the generated energy due to viscosity and magnetic resistivity, respectively, where σ is the conductivity of plasma. Here, instead, we use diffusivity, $\eta = c^2/4\pi\sigma$. Further, in the self-similar formalism, the above quantities are simplified as

$$q_{vis} = \frac{9\alpha}{4}\frac{pv_\phi^2}{rv_K}, \tag{23}$$

$$q_B = \frac{\eta}{4\pi}|\nabla\times\boldsymbol{B}|^2 = \frac{\eta}{4\pi r^2}\left[\left(\frac{1}{\sin\theta}\frac{\partial}{\partial\theta}(\sin\theta B_\phi)\right)^2 + \frac{B_\phi^2}{16}\right]. \tag{24}$$

Also, $q_- = q_{rad}$ implies energy loss through radiative cooling and we can write

$$q_{adv} = q_+ - q_- = f'q_+, \tag{25}$$

where f' is the advection parameter, which that shows what fraction of generated energy has remained in the disc at a definite polar angle; hence,

$$q_{adv} = -\frac{5 - 3\gamma}{2(\gamma - 1)}\frac{pv_r}{r}. \tag{26}$$

The advection parameter f shows the whole energy trapping the entire disc thickness: it is expressed as $f = Q_{adv}/(Q_{vis} + Q_B)$, where the latter three quantities can be achieved by vertical integration over q_{vis}, q_{adv} and q_B:

$$Q_{adv} = \int_{\theta_s}^{\pi-\theta_s} q_{adv} r\sin\theta\,d\theta, \tag{27}$$

$$Q_{vis} = \int_{\theta_s}^{\pi-\theta_s} q_{vis} r\sin\theta\,d\theta, \tag{28}$$

$$Q_B = \int_{\theta_s}^{\pi-\theta_s} q_B r\sin\theta\,d\theta. \tag{29}$$

In our system, we have seven physical quantities varying with polar angle: v_r, v_ϕ, p, ρ, c_s, B_ϕ and η. To solve an equation in these quantities, we need the seven equations (13)–(19). Using proper boundary conditions, which are introduced in the previous section, and integrating with respect to θ, we can obtain the vertical distribution of the above seven quantities numerically.

5 RESULTS

5.1 Vertical structure

5.1.1 Notification regarding non-magnetic solutions

In this section we will study the variation of dynamical quantities with the polar angle θ for a reasonable value of the squared sound velocity at the equatorial plane, c_{s0}^2 (or equivalently the gas temperature). Before that, however, we are interested in reviewing some details of the non-magnetic case. According to the original work of GXLL09, one boundary condition is required for solving equations, which was set to be $c_s = 0$ at the surface of disc, $\theta = \theta_s$. We are then able to find a solution for almost all given disc half-opening angles, $\Delta\theta[= \pi/2 - \theta_s]$, but some of those approaching nearly spherical configurations are not acceptable because of the limitation on the advection parameter, f, which must be less than unity. Let us consider equation (10) of GXLL09 and deduce v_ϕ^2 from it. Neglecting radial velocity in comparison with other velocities, we can

conclude an approximate range for the value of the squared rotational velocity:

$$v_\phi^2 \approx v_{\rm K}^2 - \frac{5}{2}c_{\rm s}^2.$$

From this equation we can determine an upper limit for $c_{\rm s}^2$: $c_{\rm smax}^2 \approx 0.4v_{\rm K}^2$, which corresponds to $v_\phi^2 \approx 0$. Thus there is an upper limit for gas pressure according to $p = \rho c_{\rm s}^2$, so the maximum pressure at $\theta = \pi/2$ becomes $p_{\rm max} \approx 0.4\rho_0 v_{\rm K}^2$. With an acceptable initial value of $c_{\rm s0}^2$ between 0 and $0.4v_{\rm K}^2$, we can start integrating from the equatorial plane instead of the surface of the disc (which was used by GXLL09); we can then conclude that the maximum disc half-thickness belongs to a maximum value of $c_{\rm s0}^2$. In this article, we follow this approach and, as we will see in the next subsection, starting integration from the other boundary, means the disc surface, is not applicable in this work at all.

5.1.2 *Solutions for the magnetic case*

Using the main equations and their boundary conditions that were introduced in last sections, equations (13)–(19), we can numerically derive the θ-direction of the distribution of physical quantities for a given radius. In our calculation we set $\gamma = 3/2$, $\alpha = 0.1$, $\eta_0 = 0.1$ and $c_{\rm s0}^2 = 0.1v_{\rm K}^2$ and the behaviour of the solution is investigated for different values of $\beta_0 (= 2p_{\rm m}/p_{\rm g})$ (zero index means at $\theta = \pi/2$). For comparison, we have presented the non-magnetic quantities as black lines in Figs 1, 2 and 3. As Figs 1–3 illustrate, the thickness of the disc decreases on increasing β_0. They show that when the magnetic field strength increases by adding β_0, the half-thickness of the discs will decrease considerably when we use identical initial

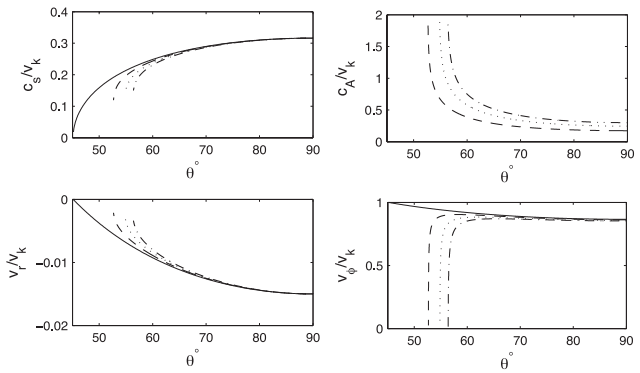

Figure 1. Self-similar solutions corresponding to $\gamma = 3/2$, $\alpha = 0.1$, $\eta_0 = 0.1$ and several values of β_0. The black line shows the solution in the non-magnetic situation: dashed, dotted and dot–dashed lines refer to $\beta_0 = 0.3, 0.6, 0.9$, while the solid line shows the corresponding quantity in the absence of magnetic field. In this figure, $v_{\rm K}$ is the Keplerian velocity.

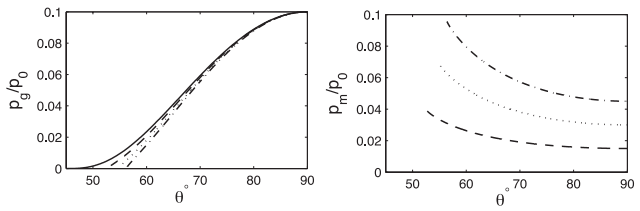

Figure 2. Self-similar solutions corresponding to $\gamma = 3/2$, $\alpha = 0.1$, $\eta_0 = 0.1$ and several values of η_0. The dashed, dotted and dot–dashed lines refer to $\beta_0 = 0.3, 0.6, 0.9$, and the solid line shows the corresponding quantity in the absence of magnetic field. In this figure, the fiducial pressure p_0 is determined by $p_0 = \rho_0 v_{\rm K}^2$.

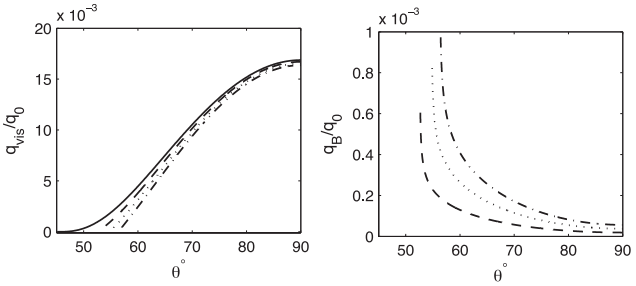

Figure 3. Variation of two forms of the dissipated energy ($q_{\rm vis}, q_B$) per unit volume of plasma, with $\gamma = 3/2$, $\alpha = 0.1$, $\eta_0 = 0.1$ and several values of β_0. The dashed, dotted and dot–dashed lines refer to $\beta_0 = 0.3, 0.6, 0.9$ and the solid line shows the energy dissipated by viscosity in the non-magnetic flow. In this figure, the fiducial dissipated energy is $q_0 = p_0 v_{\rm K}^2/r$, where $p_0 = \rho_0 v_{\rm K}^2$.

conditions (the same sound speed at $\theta = \pi/2$ and consequently the same temperature at the mid-plane). We therefore conclude that the non-magnetized disc has the maximum thickness. The top panels of Fig. 1 show the variations of $c_{\rm s}$ and $c_{\rm A}$ for some values of β_0. Obviously, they have opposite behaviour to θ, as mentioned in section 3. The top left panel of Fig. 1 displays the sound velocity, which does not change significantly near the mid-plane but at the edge of the disc it decreases with increasing β_0 until attaining zero in the non-magnetic flow. From the top right panel of Fig. 1, we see that the Alfvén velocity $c_{\rm A}(\theta)$, is minimum at $\theta = \pi/2$ and is increasing slowly except near the surface. As this plot clearly shows, β_0 effects act mainly near the edge.

In this case, the disc surface layers are non-turbulent and thus highly conducting (or non-diffusive) because the MRI is suppressed high in this situation where the magnetic and radiation pressures are larger than the thermal pressure (Lovelace, Rothstein & Bisnovatyi-Kogan 2009). The physics of the boundary layer of the disc and its corresponding physical phenomena are not the focus of this article and should be checked in future investigations. The bottom left panel shows the variation of the radial velocity, $v_r(\theta)$, with respect to the polar angle θ for the same given parameters. As we expect, for ADAFs the radial velocity is sub-Keplerian and absolute values of the radial velocity decrease with the vertical thickness of the disc, reaching zero at the surface of the disc. When the magnetic parameter, β_0, becomes larger, the absolute value of v_r decreases for a given polar angle θ and the magnitude of this reduction is more significant near the edge of the disc. It emphasizes that the maximum magnitude of radial velocity is in the equatorial region and towards the surface it tends to become zero.

The rotational velocity is shown in the bottom right panel of Fig. 1. It can be clearly seen that v_ϕ is nearly independent of θ and even β_0 in the middle region of the disc, but near the edge it changes rapidly. For the non-magnetic case we can see that the rotational velocity behaves as a monotonic function of θ, such that it is monotonically increasing from $\theta = \pi/2$ to $\theta = \pi/2 \pm \Delta\theta$. However, when the magnetic field plays an important role the rotational velocity varies differently. The magnetic field divides the disc into the two distinct regions: one region is around the mid-plane, where the rotational velocity changes slowly, while the other is near the surface, where v_ϕ is maximum at first and then decreases very fast and finally reaches zero at the surface. With decreasing β_0 the surface layer, $\Delta\theta_{\rm s}$, becomes thinner so for the limit of $\beta_0 = 0$ it tends to $\Delta\theta_{\rm s} = 0$. However, this happens at the surface boundary, where the conditions are so different from the inner region that we are not able to have an accurate solution there. Nevertheless, a mass point

rotates more slowly in a magnetized disc because it has experienced an extra magnetic force. As we expected, the radial and rotation velocities are both sub-Keplerian. Fig. 2 shows the gas and magnetic pressures scaled with a fiducial pressure, $p_0 = \rho_0 v_K^2$. The gas pressure, as we expected, behaves the same as the absolute value of the radial velocity. It peaks at $\theta = \pi/2$ and in a weak magnetic field is almost constant, but magnetic pressure, i.e. p_m in the right panel of Fig. 2, is minimum at the equatorial plane and becomes larger towards the surface. It shifts up when the magnetic parameter β_0 increases.

Fig. 3 shows variations of the scaled viscous and magnetic energy dissipation in two separate panels for the same parameters ($\gamma = 3/2$, $\alpha = 0.1$, $\eta_0 = 0.1$). It clearly shows that when the toroidal magnetic field becomes stronger, viscous dissipation decreases. However, according to the right panel of this figure, the heating process from resistivity is greater in a stronger magnetic field. Moreover, the maximum value of q_B, which occurs at the surface of the disc, is almost one order of magnitude less than the viscosity dissipation at the mid-plane, meaning $q_{B_{max}} \approx 0.1 q_{vis_{max}}$. Although the resistive dissipation can not have much effect on the advection parameter, it can cause f' to change significantly in the outer parts of the disc.

5.1.3 *The role of resistivity*

One of the prominent input parameters in our system is the magnetic diffusivity, η_0, the possible effects of which are explored in Figs 4–6. We assume that $\gamma = 3/2$, $\alpha = 0.1$ and $\beta_0 = 0.5$. The solid, dashed and dotted lines correspond to $\eta_0 = 0.05, 0.1$ and 0.2 respectively. Fig. 4 displays the sound speed c_s (top, left) and rotational velocity v_ϕ(bottom, right), normalized by the Keplerian velocity. They are

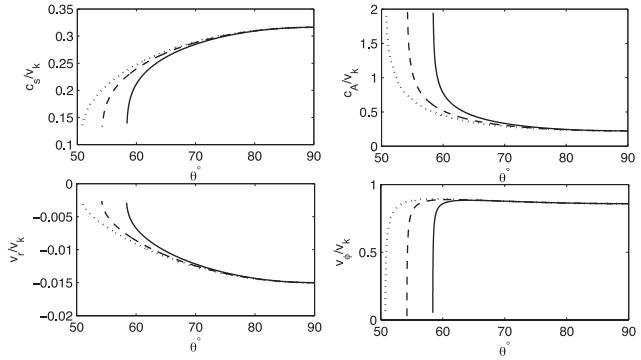

Figure 4. Self-similar solutions corresponding to $\gamma = 3/2$, $\alpha = 0.1$, $\beta_0 = 0.1$ and several values of η_0. The solid, dashed and dotted lines refer to $\eta_0 = 0.05, 0.1$ and 0.2. v_K is the Keplerian velocity.

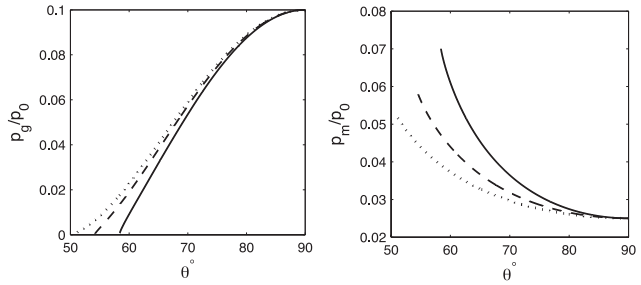

Figure 5. The profiles of the gas and magnetic pressure corresponding to $\gamma = 3/2$, $\alpha = 0.1$, $\beta_0 = 0.5$ and several values of η_0. The solid, dashed and dotted lines refer to $\eta_0 = 0.05, 0.1$ and 0.2. In this figure, the fiducial pressure p_0 is determined by $p_0 = \rho_0 v_K^2$.

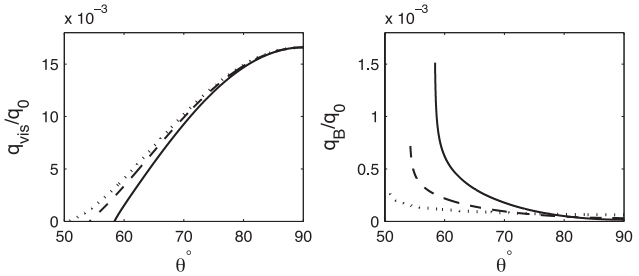

Figure 6. Variation of two forms of the dissipated energy (q_{vis}, q_B) per unit volume of plasma, corresponding to $\gamma = 3/2$, $\alpha = 0.1$, $\beta_0 = 0.5$ and several values of η_0. The solid, dashed and dotted lines refer to $\eta_0 = 0.05, 0.1$ and 0.2. In this figure, the particular dissipated energy is $q_0 = p_0 v_K^2/r$, where $p_0 = \rho_0 v_K^2$.

constant near the mid-plane but begin to change towards the surface. Radial velocity v_r is shown in the bottom left panel of Fig. 4 at a fixed equator temperature but for different values of η_0; it has a minimum value at $\theta = \pi/2$ and η_0 affects the radial velocity mainly near the edge of the disc. As is clearly shown, for higher values of the resistivity parameter the total velocity increases in the disc. In contrast, for a given θ an increase in η_0 leads to a decrease in Alfvén velocity c_A (top, right).

Fig. 5 illustrates the effects of the resistivity parameter on the gas and magnetic pressure. The left panel shows that for higher values of η_0 the gas pressure rises in the outer regions but the magnetic pressure that is shown in the right of Fig. 5 diminishes. Finally in Fig. 6 we can see how the magnetic diffusivity affects the two heating energy sources, q_{vis} (left) and q_B (right). The magnetic resistivity affects q_B explicitly, but it affects q_{vis} implicitly throughout the dynamical quantities. According to this figure, viscosity dissipation is an ascending function of η_0 in the outer regions. In spite of this, q_B is proportional to η_0: it falls off as η_0 becomes larger and for small values of η_0 it tends to be constant along the θ direction. As we can see, Ohmic heating is much smaller than viscous heating so we can ignore the role of the magnetic field in the energy equation.

5.2 Thickness of the flow

In this section we will explore how the physical input parameters of the system affect the thickness of the flow. At first, we will review the approach that is usually used for α discs and then explain the special method applied by GXLL09, with more details for the magnetized case.

5.2.1 *The usual way for estimating of the flow thickness*

At first we consider the usual approximation for the thickness of flow, which is based on the α-prescription, meaning that $\nu = \alpha c_s H$ where $H = c_s/\Omega_K$ or $H/r = c_s/v_K$ and H is the half-thickness of the disc. This is the result of hydrostatic equilibrium; it means the gravitational force and the pressure force are balanced with each other in the vertical direction:

$$\frac{1}{\rho}\frac{\partial p}{\partial z} + \frac{\partial \psi}{\partial z} = 0, \tag{30}$$

where ψ is the gravitational potential in cylindrical coordinates and can be written as $\psi = -GM/(r^2 + z^2)^{1/2}$. Now, using some approximations we can estimate the half-thickness of disc in this way: $\partial p/\partial z \approx -p_0/H$, $\rho \approx \rho_0$ (the zero index shows the value of a quantity at the equatorial plane), $\partial \psi/\partial z \approx GMH/r^3 = \Omega_K^2 H$

and the sound velocity is $c_{s0} = (p_0/\rho_0)^{1/2}$. As we mentioned in Section 5.1.1, the squared sound velocity cannot exceed more than $0.4v_K^2$, so $H/r \leq \sqrt{0.4} = 0.63$ in the non-magnetic flow.

In the presence of a toroidal magnetic field, the magnetic force is added to the vertical component of the motion equation:

$$\frac{\partial p}{\partial z} + \frac{B_\phi}{4\pi}\frac{\partial B_\phi}{\partial z} + \rho\frac{\partial \psi}{\partial z} = 0. \quad (31)$$

We can use the magnetic pressure, $p_m = B_\phi^2/8\pi$, which is usually (e.g. Narayan & Yi 1995b) assumed to be proportional to the gas pressure p, i.e. $p_m = \beta p$, so with the previous assumptions one can easily achieve $H/r = (1+\beta)^{1/2}c_s/v_K$. Therefore the half-thickness of the disc increases when we add the influence of the magnetic field on the structure of the accretion flow. We will show that this conclusion is not valid if we take into account the induction equation. In the following subsection, we study several details that can affect the thickness of the disc in the presence of a magnetic field. For simplicity, as we noted in the Introduction, in this study a toroidal configuration for the magnetic field is assumed.

5.2.2 *The thickness of the magnetized flow*

As we noted in the Introduction, the aim of this article is to revisit the vertical structure of hot accretion flows when the magnetic field has an important role. Also, we expand the equations in spherical coordinates. So the study of the vertical structure in magnetized cases is quite complicated and different from the non-magnetized case, since the induction equation should be taken into account.

As mentioned in Section 5.1.1, the solution shows that the sound velocity decreases from the mid-plane towards the surface and becomes zero at the surface of a non-magnetized disc. However, in the presence of a magnetic field, we first need to consider equation (13):

$$v_\phi^2 = v_K^2 - \frac{1}{2}v_r^2 - \frac{5}{2}c_s^2 - \frac{1}{4}c_A^2, \quad (32)$$

so the rotational velocity depends not only on c_s but also on c_A. Here, the Alfvén velocity has a crucial role in determination of the disc thickness. As we saw in the previous section in Figs 1 and 4, the sound and Alfvén velocities have different behaviours; therefore v_ϕ can have a non-monotonic behaviour from the equatorial plane towards the edge of the flow. At first, it increases because of decreasing c_s^2, but c_A^2 is still too small to affect v_ϕ^2 considerably. Somewhere between the mid-plane and the surface, c_A^2 becomes large enough (comparable with c_s^2) and makes the rotational velocity start to reduce until it is zero at the disc surface. Thus, we must consider the influences associated with the Alfvén velocity's behaviour.

Although there are strict limitations on what can be discussed regarding the numerical solutions, we can consider a special point to help us to determine the general behaviour of the solution. The symmetry assumption about the equatorial plane hints that this point is $\theta = \pi/2$. There are two possible symmetry configurations for the toroidal magnetic field with respect to the equatorial plane, even and odd symmetry. Nevertheless, both of them lead to the same result, because B_ϕ^2 is important here and it is an even function and also minimum for both symmetries.

The behaviour of the magnetic field inside the disc depends on $\partial^2 B_\phi^2/\partial\theta^2 = \Delta B_\phi^2$ at the equatorial plane. From the induction equation (see Appendix), we can obtain

$$\left.\frac{\partial^2 B_\phi^2}{\partial\theta^2}\right|_{90^\circ} = \left(\frac{13}{8} + \frac{9\alpha}{4\eta_0}\right)B_{\phi 0}^2 > 0. \quad (33)$$

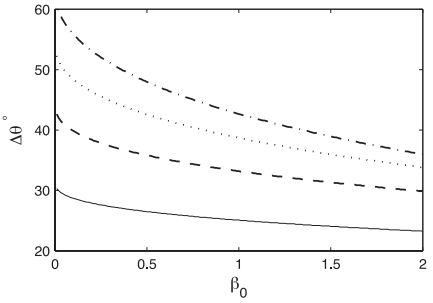

Figure 7. The disc's half-opening angle, $\Delta\theta$, as a function of the magnetic field strength parameter at the equatorial plane, β_0, for $\gamma = 3/2$, $\alpha = 0.1$, $\eta_0 = 0.1$ and various values of the equatorial square sound velocity; the solid, dashed, dotted and dot–dashed lines represent $c_{s0}^2/v_K^2 = 0.05,\ 0.10,\ 0.15$ and 0.20.

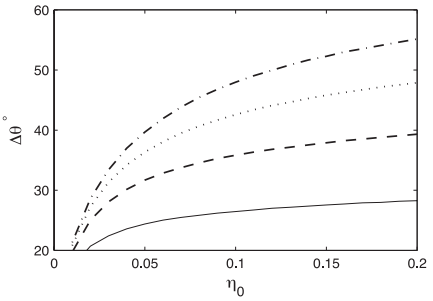

Figure 8. The disc half-opening angle, $\Delta\theta$, as a function of the resistivity parameter, η_0, for $\gamma = 3/2$, $\alpha = 0.1$, $\beta_0 = 0.5$ and various values of the equatorial square sound velocity; the solid, dashed, dotted and dot–dashed lines represent $c_{s0}^2/v_K^2 = 0.05,\ 0.10,\ 0.15$ and 0.20.

The above relation indicates that B_ϕ^2 is minimum at the mid-plane. On the other hand, if ΔB_ϕ^2 becomes larger, B_ϕ^2 will increase more rapidly and make the disc thiner. According to the last relation, ΔB_ϕ^2 is directly proportional to $B_{\phi 0}^2 = 8\pi\beta_0 c_{s0}^2$ and depends directly on α but inversely on η_0.

Having an inverse relationship between the disc thickness and ΔB_ϕ^2, an increase in β_0 or α leads to a decrease in the disc thickness, but it increases with increasing η_0.

We can see the effects of β_0 and η_0 in Figs 7 and 8. As we expect before, Fig. 7 shows that by increasing the β_0 parameter, the disc thickness decreases and this effect is stronger for a high temperature of the flow. However, we can say that the magnetic force in the vertical direction compresses the disc. Liffman & Bardou (1999) and Campbell & Heptinstall (1998) also noted compression of disc in the height direction through the effect of a toroidal magnetic field. From Fig. 8, it is seen that the magnetic resistivity has a direct effect on the thickness of the flow: when it is increased, the disc thickness also increases.

5.3 Advective parameter

As we mentioned before, in this work, to determine the advective parameter we first solve the system of differential equations and, after finding dynamical quantities in the fluid, we can specify f according to equations (27), (28) and (29) and the relation $f = Q_{adv}/(Q_{vis} + Q_B)$. It is seen that in trhe case of a magnetic field that tends to compress the fluid, much more advecting energy can be saved in a disc with lower thickness, in comparison with non-magnetic flow. For example, we can see (for $\gamma = 4/3$) that $f = 0.1$ in a

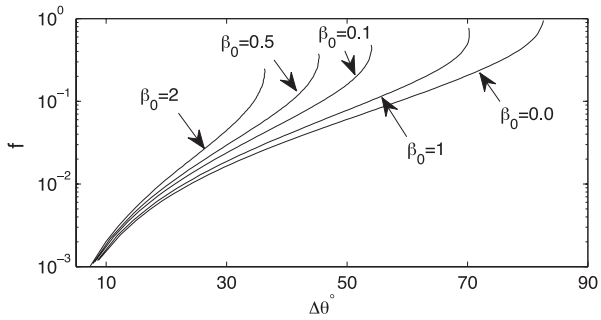

Figure 9. Variation of the advection factor, f, with the disc half-opening angle, $\Delta\theta$, for $\gamma = 3/2$, $\alpha = 0.1$, $\eta_0 = 0.1$ and various value of β_0.

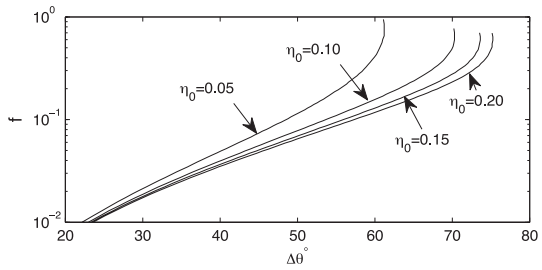

Figure 10. Variation of the advection factor, f, with the disc half-opening angle, $\Delta\theta$, for $\gamma = 3/2$, $\alpha = 0.1$, $\beta_0 = 0.1$ and various value of η_0.

non-magnetic flow with $\Delta\theta = 0.4\pi = 72^\circ$, while the same f, ($f = 0.1$) is achieved in a thinner magnetized flow with $\Delta\theta = 0.33\pi = 59.4^\circ$ and $\beta_0 = 0.1$. It helps somewhat that the previous suggestion of slim discs that are neither thin nor thick retains its validity.

In Fig. 9, f is plotted as a function of β_0 for a fixed value of c_{s0}. It shows that much more energy can be advected in the stronger magnetic field that exists in a thinner disc; in a hotter disc (i.e. with greater sound velocity), advection will be intensified.

The profile of the energy advection factor, f, for various values of magnetic resistivity parameter η_0 is presented as a function of the disc half-opening angle in Fig. 10. It demonstrates that energy advection decreases inversely with η_0 for fixed disc thickness.

5.4 Bernoulli parameter

In stationary, inviscid flows with no energy sources or losses, the quantity (Abramowicz, Lasota & Igumenshchev 2000)

$$Be_0 = W + \frac{1}{2}V^2 + \Phi \tag{34}$$

is constant along each individual streamline but, in general, is different for different streamlines. This quantity is called the Bernoulli constant. Here, W is the specific enthalpy, V is the velocity (all three components included) and Φ is the gravitational potential:

$$Be_0 = \frac{1}{2}\left(v_r^2 + v_\phi^2\right) - \frac{GM}{r} + \frac{\gamma}{\gamma - 1}\frac{p}{\rho}. \tag{35}$$

Obviously, a particular streamline may end up at infinity only if $Be_0 > 0$ along it. The existence of streamlines with $Be_0 > 0$ is therefore a necessary condition for outflows in stationary inviscid flows with no energy sources or losses and $Be_0 < 0$ for all streamlines is a sufficient condition for the absence of outflows. However, $Be_0 > 0$ is not a sufficient condition for outflows. In all viscous flows, Be_0 is not constant along individual streamlines. For self-similar solutions,

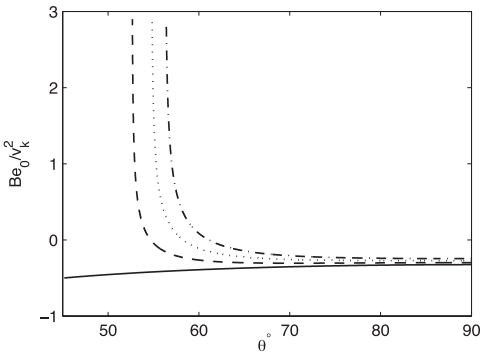

Figure 11. Bernoulli parameter with respect to θ for different value of β_0. The black line corresponds to $\beta_0 = 0$, the dashed line to $\beta_0 = 0.3$, the dotted line is for $\beta_0 = 0.6$ and the dot–dashed line is for $\beta_0 = 0.9$ ($c_{s0}^2 = 0.1v_K^2$ is the boundary condition at $\theta = \pi/2$ and $\gamma = 3/2$).

Be_0 is a function of r^{-1} so it cannot be a constant value at all. Hence, the so-called 'Bernoulli parameter' is introduced: $\widetilde{Be}_0 = Be_0/V_K^2$.

In the presence of a magnetic field, an extra term needs to be added to the Bernoulli function (Fukue 1990). Since the Bernoulli equation is based on energy conservation along each streamline, in the magnetic case the total energy of the fluid is included in the magnetic energy in addition to the other previous forms of energies in equation (35). Thus, the Bernoulli function of magnetized flow becomes

$$Be(r,\theta) = \frac{1}{2}\left(v_r^2 + v_\phi^2\right) - \frac{GM}{r} + \frac{\gamma}{\gamma - 1}\frac{p}{\rho} + \frac{B_\phi^2}{4\pi\rho}. \tag{36}$$

For the self-similar model it is simplified as $Be(r,\theta) = Be(\theta)v_K^2$:

$$Be(\theta) = \frac{1}{2}\left[v_r^2(\theta) + v_\phi^2(\theta)\right] - 1 + \frac{\gamma}{\gamma - 1}c_s^2(\theta) + c_A^2(\theta). \tag{37}$$

As we see from Fig. 11, without magnetic field the Bernoulli function in ADAFs with low viscosity is negative, but in the presence of magnetic field it can achieve a positive value close to the surface. This means that GXLL09 solutions without magnetic field cannot describe the existence of wind and outflow.

6 DISCUSSION AND CONCLUSION

The vertical structure of a hot accretion flow is still an open problem. Hence in this article, following the work of GXLL09, we have considered a two-dimensional axisymmetric advection-dominated accretion flow in spherical coordinates with a toroidal magnetic field. We have concentrated on studying possible effects of the magnetic field and its corresponding resistivity on the radial and vertical accretion structure. With a self-similar solution along the radial direction and the proper boundary conditions using reflection symmetry in the equatorial plane of the disc, we have constructed the structure of the disc along the θ direction explicitly.

In this article we used the induction equation for a resistive flow in order to complete the system of basic equations of fluid dynamics. We assumed $\beta[= 2\frac{p_m}{p_g}]$ to be a function of θ, while in previous articles (Akizuki & Fukue 2006; Abbassi et al. 2008, 2010) it was adopted as a constant. As a result, we could find new solutions for the dynamical quantities of ADAFs in the presence of a toroidal magnetic field, B_ϕ. The stationary solutions we found indicate that even a weak toroidal field at the mid-plane can grow significantly near the edge and cause a significant change in the surface layers. Moreover, the main purpose of this article is to investigate how the

vertical thickness of the disc changes in the presence of a toroidal magnetic field, B_ϕ. We considered an even configuration of B_ϕ and found that it has a squeezing effect on the disc structure, where the disc thickness is reduced compared with the non-magnetic case. In fact, the squeezing effect of B_ϕ counterbalances the thickening of the disc generated by advection (Shadmehri & Khajenabi 2005). Our conclusions are opposite to those of Wang et al. (1990) (for the odd symmetry case) because the envisioned models are different in the two cases. Wang et al. assume a relatively thin disc ($H < r$), whereas we consider a thick disc, $H \sim R$. The solution presented in this article is in good agreement with that presented by Mosallanezhad, Abbassi & Beiranvand (2014), for which they used the same physical method and assumptions. Their solutions indicate that the outflow region, where the radial velocity becomes positive at a certain inclination angle θ_0, always exists. They have shown that a stronger toroidal magnetic field leads to a smaller inclination angle, which means a thinner disc.

The complex behaviour of the flow depends on the input parameters of the problem and is explored in detail in this article. However, a complete analysis is needed to complete our model, including a detailed analysis of the edge of the disc. We point out that the accretion outflow solutions are unstable near the outer edge and outside the accretion flow. Further and more detailed study should be made of the wind region solution and its interaction with the large-scale magnetic field. The present results lend strong support to the suggestion that the magnetic field has an important role in the vertical structure of hot flows and magnetically channelled wind. Also, we have noted that the diffusion properties of the magnetically dominated corona have never been investigated and it would be good if these were tested in future investigations.

ACKNOWLEDGEMENTS

The authors are particularly grateful to Richard Lovelace, Mohsen Shadmehri and Fu-Guo Xi for their discussions and useful suggestions. We also appreciate the referee's thoughtful and constructive comments, which clarified some points in the early version of the article. This work was supported by Ferdowsi University of Mashhad under the grant 3/27130 (1392/03/16).

REFERENCES

Abbassi S., Ghanbari J., Najjar S., 2008, MNRAS, 388, 663
Abbassi S., Ghanbari J., Ghasemnezhad M., 2010, MNRAS, 409, 1113
Abramowicz M. A., Czerny B., Lasota J. P., Szuszkiewicz E., 1988, ApJ, 332, 646
Abramowicz M. A., Lasota J.-P., Igumenshchev I. V., 2000, MNRAS, 314, 775
Akizuki C., Fukue J., 2006, PASJ, 58, 469
Balbus S. A., Hawley J. F., 1991, ApJ, 376, 214
Bisnovatyi-Kogan G. S., Blinnikov S. I., 1976, Sov. Astron. Lett., 2, 191
Bisnovatyi-Kogan G. S., Ruzmaikin A. A., 1976, Ap&SS, 42, 401
Campbell C. G., Heptinstall P., 1998, MNRAS, 299, 31
Fukue J., 1990, PASJ, 42, 793
Ghanbari J., Salehi F., Abbassi S., 2007, MNRAS, 381, 159
Gu W.-M., Xue L., Liu T., Lu J.-F., 2009, PASJ, 61, 1313
Kaburaki O., 2000, ApJ, 531, 210
Kato S., Fukue J., Mineshige S., 2008, Black-Hole Accretion Disks – Towards a New Paradigm. Kyoto Univ. Press, Kyoto
Khesali A., Faghei K., 2009, MNRAS, 398, 1361
Liffman K., Bardou A., 1999, MNRAS, 309, 443
Lovelace R. V. E., Mehanian C., Mobarry C. M., Sulkanen M. E., 1986, ApJS, 62, 1
Lovelace R. V. E., Wang J. C. L., Sulkanen M. E., 1987, ApJ, 315, 504
Lovelace R. V. E., Rothstein D. M., Bisnovatyi-Kogan G. S., 2009, ApJ, 701, 885
Lynden-Bell D., 1969, Nature, 223, 690
Manmoto T., Mineshige S., Kusunose M., 1997, ApJ, 489, 791
Mosallanezhad A., Abbassi S., Beiranvand N., 2014, MNRAS, 437, 3112
Narayan R., Yi I., 1994, ApJ, 428, L13
Narayan R., Yi I., 1995a, ApJ, 444, 231
Narayan R., Yi I., 1995b, ApJ, 452, 710
Novikov I. D., Thorne K. S., 1973, in DeWitt C., DeWitt B., eds, Black Holes. Gordon & Breach, New York, p. 345
Papaloizou J. C. B., Terquem C., 1997, MNRAS, 287, 771
Shadmehri M., 2004, A&A, 424, 379
Shadmehri M., Khajenabi F., 2005, MNRAS, 361, 719
Shakura N. I., 1972, Astron. Zh., 49, 921 (1973, Sov. Astron., 16, 756)
Shakura N. I., Sunyaev R. A., 1973, A&A, 24, 337
Wang J. C. L., Sulkanen M. E., Lovelace R. V. E., 1990, ApJ, 355, 38
Watarai K.-Y., Fukue J., Takeuchi M., Mineshige S., 2000, PASJ, 52, 133
Xue L., Wang J., 2005, ApJ, 623, 372

APPENDIX A

We seek a proper boundary for $c_{\rm A}^2$, but before that we need to investigate the behaviour of $c_{\rm A}^2$ from the equatorial plane towards disc surface. For this purpose we refer to the induction equation:

$$\frac{\partial B_\phi}{\partial t} = \frac{1}{r}\frac{\partial}{\partial r}\left[\eta\frac{\partial}{\partial r}(rB_\phi) - rv_r B_\phi\right] + \frac{1}{r^2}\frac{\partial}{\partial\theta}\left[\eta\left(B_\phi\cot\theta + \frac{\partial B_\phi}{\partial\theta}\right)\right]. \tag{A1}$$

We suppose that $\partial B_\phi/\partial t = 0$ and then, by multiplying by $B_\phi/4\pi\rho$, we have (after multiplication and some simplification)

$$\frac{3}{8}\left(\frac{1}{2} - \frac{3\alpha}{\eta_0}\right)c_{\rm s}^2 B_\phi^2 + \frac{\partial c_{\rm s}^2}{\partial\theta}\left(B_\phi^2\cot\theta + \frac{1}{2}\frac{\partial B_\phi^2}{\partial\theta}\right) + c_{\rm s}^2\left[-\frac{B_\phi^2}{\sin\theta^2} + \frac{1}{2}\frac{\partial B_\phi^2}{\partial\theta}\cot\theta + \frac{1}{2}\frac{\partial^2 B_\phi^2}{\partial\theta^2} - \frac{1}{4B_\phi^2}\left(\frac{\partial B_\phi^2}{\partial\theta}\right)^2\right] = 0. \tag{A2}$$

This relation in the equatorial plane ($\theta = \pi/2$), where $\partial/\partial\theta = 0$, converts to

$$\frac{\partial^2 B_\phi^2}{\partial\theta^2} = \frac{13}{8}\left(1 + \frac{18\alpha}{13\eta_0}\right)B_\phi^2 > 0. \tag{A3}$$

It is therefore obvious that B_ϕ^2 must be a minimum in the equator of the disc.

This paper has been typeset from a TEX/LATEX file prepared by the author.